Statistical Time Series Methods for Multicopter Fault Detection and Identification

Airin Dutta PhD Student
Michael McKay PhD Student
Fotis Kopsaftopoulos Assistant Professor
Farhan Gandhi Redfern Professor, Director

Center for Mobility with Vertical Lift (MOVE)
Rensselaer Polytechnic Institute, Troy, NY

ABSTRACT

This work presents the use of statistical time series methods to detect and identify rotor failures in multicopters. A concise overview of the development of various time series models using scalar or vector signals, statistics, and fault detection and identification methods has been provided. The statistical methods employed in this study are based on parametric time series representations and response-only signals of the aircraft state, as the external excitation is non-observable. The comparative assessment of the effectiveness of scalar and vector statistical models and several residual-based fault identification methods are presented in the presence of external disturbances, such as various levels of turbulence and uncertainty, and for different rotor failure scenarios. Fault identification (classification) of different rotor failures has been performed upon post-failure controller compensated steady state signals. Vector models, being more elaborate models than their scalar counterparts, exhibit superior performance in fault identification. On the other hand, residual uncorrelatedness method have greater capability to differentiate between the different rotor failures than residual variance method.

NOTATION

α	:	Type I risk level
β	:	Type II risk level
γ	:	Autocorrelation
τ	:	Lag
σ^2	:	Residual variance
$\boldsymbol{\Sigma}$	:	Residual covariance matrix
ARMA	:	AutoRegressive Moving Average
$E\{\cdot\}$	:	Statistical expectation
PE	:	Prediction error
ARX	:	AutoRegressive with eXogenous excitation
PSD	:	Power spectral density
BIC	:	Bayesian information criterion
RSS	:	Residual sum of squares
FRF	:	Frequency response function
ACF	:	Auto-covariance function
iid	:	Identically independently distributed
SPP	:	Samples per parameter
OLS	:	Ordinary least squares
UAV	:	Unmanned aerial vehicle
WLS	:	Weighted least squares
SPRT	:	Sequential probability ratio test
SSS	:	Signal sum of squares
AR	:	Scalar AutoRegressive model
VAR	:	Vector AutoRegressive model
e-VTOL	:	electric vertical take-off and landing

Presented at the Vertical Flight Society International Powered Lift Conference, San Jose, California, Jan 21-23, 2020.

INTRODUCTION

Multicopters, being capable of hovering and vertical take-off and landing, have attracted the interest of the community with respect to both commercial and defense applications over the last decade. Given the increasing interest and widespread use of these vehicles in a number of important arenas, early fault detection and identification of such systems are critical in order to ensure and improve their overall safety, operation and reliability. Rotorcraft are complex systems that exhibit strong dynamic coupling between rotors, fuselage, and control inputs, along with time-varying and cyclo-stationary behavior. As a result, they face certain system modeling and fault detection and identification challenges that are not present in fixed-wing aircraft. These issues, as well as potential solutions, have been explored in the recent literature.

An algorithm for online detection of motor failure using only inertial measurements and control allocation by an exact redistributed pseudo-inverse method for octacopters has been demonstrated by Frangenberg et al. (Ref. 1). Heredia and Ollero (Ref. 2) have addressed sensor fault identification in small autonomous helicopters using Observer/Kalman Filter identification. Fault tolerant control for multi-rotors (Refs. 3, 4), as well as various fault diagnosis methods related to analytical models, signal processing, and knowledge-based approaches for helicopters have also been proposed (Refs. 5–7).

Statistical time series methods have been used to detect various fault types in aircraft systems due to their simplicity, efficient handling of uncertainties, no requirement of physics-based models, and potential for applicability to different operating conditions (Refs. 8–11). Dimogianopoulos et

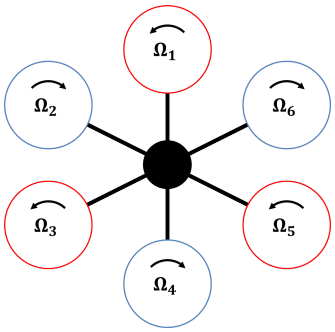

Fig. 1: Schematic representation of a regular hexacopter

al. (Ref. 12) have demonstrated the effectiveness of two statistical schemes based on Pooled Non-Linear AutoRegressive Moving Average with eXogenous excitation (P-NARMAX) to detect and isolate faults for aircraft systems under different flight conditions, turbulence levels, and fault types and magnitudes. The first method models the pilot input and aircraft pitch rate relationship, while the second approach models the relationship between horizontal and vertical acceleration, angle of attack and pitch rate signals in fixed-wing aircraft.

The objective of this paper is the presentation of a robust framework for fault identification (FDI) in multicopters using statistical time series methods based on aircraft response-only signals in the presence of external disturbances, such as turbulence, and uncertainty. This work is a continuation of a recent prior work with the addition of modeling different faulty states of the aircraft to identify rotor failures from the post failure fault-compensated signals by statistical methods (Ref. 6). FDI is the first and important step to implement an active fault tolerant control system that achieves real-time and effective control allocation redistribution or reconfiguration of the vehicle to complete safe flight in the event of rotor failure.

HEXACOPTER MODEL AND DATA GENERATION

Physics-Based Modeling of Multicopter System

A flight simulation model has been developed for a regular hexacopter (Fig. 1) using summation of forces and moments to calculate aircraft accelerations. This model is used as the main source of simulated data under varying operating and environmental conditions, as well as different fault types. Rotor loads are calculated using Blade Element Theory coupled with a 3×4 Peters-He finite state dynamic wake model (Ref. 13). This model allows for the simulation of abrupt rotor failure by ignoring the failed rotor inflow states and setting the output rotor forces and moments to zero.

A feedback controller is implemented on the nonlinear model to stabilize the aircraft altitude and attitudes, as well as track desired trajectories written in terms of the aircraft velocities. This controller is designed at multiple trim points, with gain scheduling between these points to improve performance throughout the flight envelope.

The state vector consists of the 12 rigid body states and is defined in Eq. 1.

$$\mathbf{x} = \begin{Bmatrix} X & Y & Z & \phi & \theta & \psi & u & v & w & p & q & r \end{Bmatrix}^T \quad (1)$$

The input vector is comprised of the first four independent multirotor controls for collective, roll, pitch and yaw and is defined in Eq. 2:

$$\mathbf{u} = \begin{Bmatrix} \Omega_0 & \Omega_R & \Omega_P & \Omega_Y \end{Bmatrix}^T \quad (2)$$

The control architecture is illustrated in Fig. 2 and detailed in Ref. 3. This control design has been demonstrated to perform well even in the event of rotor failure, with no adaptation in the control laws themselves.

Data Generation for Model Identification

A continuous Dryden wind turbulence model (Ref. 14) has been implemented in the flight simulation model. The Dryden model is dependent on altitude, length scale, and turbulence intensity and outputs the linear and angular velocity components of continuous turbulence as spatially varying stochastic signals. The proper combination of these parameters determines the severity of the turbulence, *i.e.,* light, moderate and severe.

In this system, the altitude is set to 5 m and the length scale (hub-to-hub distance of the hexacopter) is equal to 0.6096 m (2 ft). The data sets for the various aircraft states are generated through a series of simulations under different turbulence levels (light, moderate and severe) both for the healthy aircraft as well as under different fault types, such as failure of front and side rotors. For a summary of the generated data sets, see Table 1. The time series (signals) of the hexacopter attitudes (aircraft states) for the healthy state, as well as under the different fault types, *i.e.* complete failure of front or side rotors, provide useful insight into the dynamics of the system. The rotor failures addressed in this work are: front rotor (rotor 1), right-side rotor (rotor 2), and left-side rotor (rotor 6).

WORKFRAME OF STATISTICAL TIME SERIES FOR FAULT DETECTION AND IDENTIFICATION

Let Z_0 designate the aircraft under consideration in its healthy state, and Z_1, Z_2, and Z_6 the aircraft under rotor 1,2, or 6 failure. Z_u designates the unknown (to be determined) state of

Table 1: Simulation data under the considered flight states.

Aircraft state	Number of data sets for turbulence levels		
	Light	Moderate	Severe
Healthy	20	20	20
Rotor failure (1)	20	20	20
Rotor failure (2)	20	20	20
Rotor failure (6)	20	20	20
Sampling frequency: $f_s = 1000$ Hz			
Signal length in samples: 60000 (60 s)			

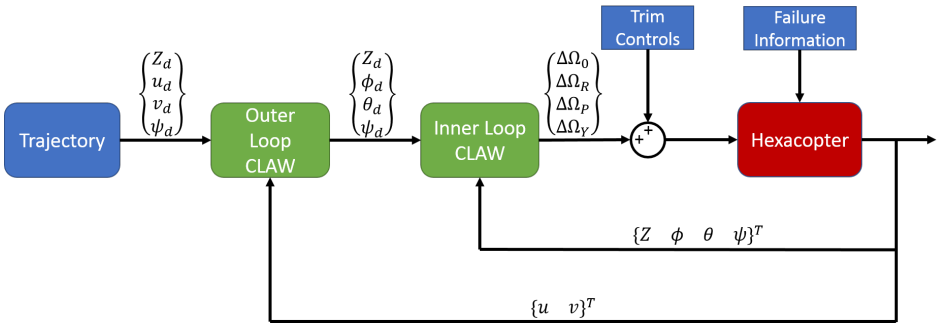

Fig. 2: Controller Block Diagram

the aircraft. Statistical time series modeling is based on discretized response signals $y[t]$[1] (for $t = 1,2,\ldots,N$) which are the aircraft states. N denotes the number of samples and the conversion from discrete normalized time to analog time is based on $(t-1)T_s$, with T_s being the sampling period. The response signals are represented by Z and subscript $(0,1,2,6,u)$ is used to denote the corresponding state of the aircraft that produced the signals. The initial sampling frequency (F_s) for the signals is chosen such that the frequency range of interest is $0-500$ Hz. After a preliminary investigation, the signals are downsampled to the final frequency bandwidth of $0-50$ Hz.

The signals generated from simulation are analyzed by parametric or non-parametric statistical time series methods and proper models are fitted and validated. Such models are identified for the above mentioned cases and denoted by M_0, M_1, M_2, M_6 in the baseline phase. Fault detection is based on binary statistical hypothesis testing (Ref. 15) that compares the residual properties (known as characteristic quantity, Q) generated from Z_u in each inspection phase with that available from baseline models. The characteristic quantities obtained from the corresponding residual series are designated as $Q_{0u}, Q_{1u}, Q_{2u}, Q_{6u}$. The characteristic quantities obtained using the baseline data records are designated as $Q_{VV}(V = 0,1,2,6)$. The first subscript designates the model employed, while the second the aircraft state corresponding to the currently used response signal(s). The design of a binary statistical hypothesis test is generally based on the probabilities of type I (false alarm) and type II (missed faults) error probabilities, represented by α and β, respectively.

The general workframe for fault detection and identification via statistical time series methods is illustrated in Fig. 3. As the flight commences, the current (unknown) signals are filtered through a healthy model of the aircraft and the properties of residual sequences generated are statistically compared with the nominal value (characteristic quantity) to determine when a rotor failure takes place. Due to rotor failure, the aircraft signals become non-stationary, until the controller compensates for the fault. The variance of the signals is monitored to ascertain that they have reached stationary state as the statistical models for different rotor failures have been estimated with fault-compensated signals. Next, these faulty signals are filtered through the faulty models to identify which rotor has failed by multiple binary hypothesis tests.

[1] A functional argument in parentheses designates function of a real variable; for instance $x(t)$ is a function of analog time $t \in \mathbb{R}$. A functional argument in brackets designates function of an integer variable; for instance $x[t]$ is a function of normalized discrete time $(t = 1,2,\ldots)$.

BASELINE MODELING OF HEALTHY AND FAULTY STATES

The aircraft signals for roll, pitch, and yaw generated via a series of simulations of forward flight of the hexacopter under turbulence (light, moderate and severe levels) for healthy and different faulty states are used in the model identification stage that subsequently drives the fault detection and identification tasks.

In the present scenario, the data sets obtained are in the form of response-only signals with the excitation $x[t]$ assumed to be a white (uncorrelated) signal induced by atmospheric turbulence. That is $\gamma_{xx}[\tau] = 0$ for $\tau \neq 0$, where γ_{xx} denotes the AutoCorrelation Function (ACF) and τ the ACF time lag, given as:

$$\gamma_{xx}[\tau] = E\{x[t] \cdot x[t+\tau]\} \tag{3}$$

Parametric Identification via Time Series Models

Scalar AR Identification Method A single signal obtained from a healthy flight simulation is parametrized to form a scalar (univariate) AutoRegressive (AR) time series model (Ref. 16):.

$$y[t] + \sum_{i=1}^{na} a_i \cdot y[t-i] = e[t], \quad e[t] \sim iid\ \mathcal{N}(0, {\sigma_e}^2) \tag{4}$$

with a_i and na designating the AR parameters and model orders, respectively; iid stands for identically independently distributed, and $\mathcal{N}(\cdot,\cdot)$ denotes a univariate normal distribution with the indicated mean and variance, respectively. In Eq. 4, $e[t]$ coincides with the one-step-ahead-prediction error and is also referred as the model residual or innovations sequence (Refs. 16, 17).

The identification of parametric time series models is comprised of two main tasks: parameter estimation and model order selection. The parameters for the AR model can been

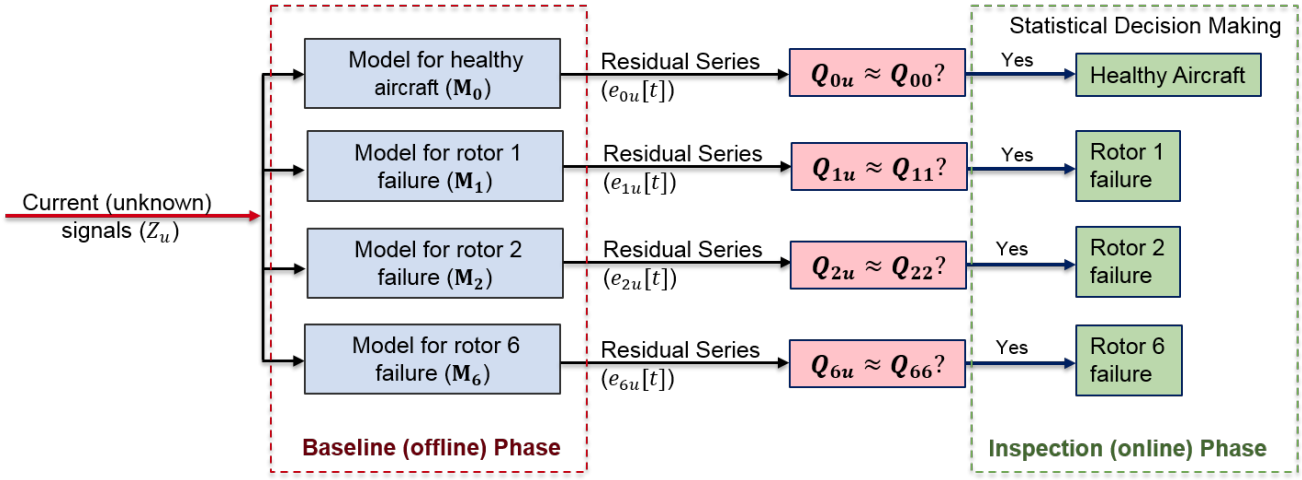

Fig. 3: General workframe of statistical time series methods for fault detection and identification.

estimated by minimization of the Least Squares (LS) criterion (Refs. 17, 18), whereas the model order selection is achieved based on the examination of the Bayesian Information Criterion (BIC) (Refs. 17, 18) (Eq. 5) and Residual sum of Squares over Signal Sum of Squares Criterion (RSS/SSS) (Eq. 6). The former is a statistical criterion that penalizes model complexity (order, and hence the number of free parameters) as a counteraction to a decreasing model fit criterion. The latter determines the predictive capability of the model.

$$BIC = \ln \sigma_e^2 + (d \cdot \ln N)/N \tag{5}$$

$$RSS/SSS = \frac{\sum_{t=1}^{N} e[t]^2}{\sum_{t=1}^{N} y[t]^2} \tag{6}$$

In Eq. 5, σ_e^2 is the variance of the residuals, d denotes the number of parameters to be estimated for the model and N denotes the number of samples used for estimation.

Vector AR Identification Method Vector AutoRegressive (VAR) models employ s-dimensional signals, *i.e.*, the aircraft states in the present study, for multivariate (s-variate) time series modeling (Refs. 19, 20). Though they bear striking resemblance to their univariate or scalar counterparts, they have a much richer structure and typically require multivariate statistical decision making procedures. The univariate response signal $y[t]$ of Eq. 4 is replaced by an s-variate vector $\boldsymbol{y}[t]$[2], hence the VAR(na) model is of the following form:

$$\boldsymbol{y}[t] + \sum_{i=1}^{na} \boldsymbol{A}_i \cdot \boldsymbol{y}[t-i] = \boldsymbol{e}[t] \tag{7}$$
$$\text{with} \quad \boldsymbol{e}[t] \sim \text{iid}\, \mathcal{N}(\boldsymbol{0}, \boldsymbol{\Sigma}), \quad \boldsymbol{\Sigma} = E\{\boldsymbol{e}[t] \cdot \boldsymbol{e}^T[t]\}$$

with $\boldsymbol{A}_i$ $(s \times s)$ designating the i-th AR matrix, $\boldsymbol{e}[t]$ $(s \times 1)$ the model residual sequence characterized by the non-singular and generally non-diagonal covariance matrix $\boldsymbol{\Sigma}$, n the AR order, and $E\{\cdot\}$ statistical expectation. Given the attitude signal measurements $\boldsymbol{y}[t]$ $(t = 1, 2, \ldots, N)$, the estimation of the VAR parameter vector $\boldsymbol{\theta}$ comprising all AR matrix elements ($\boldsymbol{\theta} = \text{vec}([\boldsymbol{A}_1\ \boldsymbol{A}_2\ \ldots\ \boldsymbol{A}_{na}])$) and the residual covariance matrix ($\boldsymbol{\Sigma}$) is accomplished via linear regression schemes based on minimization of the Ordinary Least Squares (OLS) or the Weighted Least Squares (WLS) criterion (Refs. 17, 18). The modeling procedure involves the successive fitting of VAR(na) models for increasing AR order, na, until an adequate model is achieved. The model order is chosen by replacing the variance of residuals for the scalar case by the trace of the residual covariance matrix, $\boldsymbol{\Sigma}$ (Ref. 9).

RESIDUAL BASED FAULT DETECTION AND IDENTIFICATION

For fault detection and identification, model residual based methods use functions of the residual sequences which are obtained by driving the current signal(s) (Z_u) through the models estimated in the baseline phase for the healthy aircraft (M_o) and different fault types (M_1, M_2, M_6). The key idea is that the residual sequence obtained by a model that truly reflects the current state of aircraft possesses certain distinct properties which are distinguishable from that obtained from the other models.

Let M_V designate the model representing the structure in its V state ($V = 0, 1, 2, 6$), where the subscript "0" denotes healthy state, and $1, 2, 6$ designate the rotor which has failed in the faulty state. The residual series obtained by driving the current signal(s) (Z_u) through each one of the aforementioned models are designated as $e_{0u}[t], e_{1u}[t], e_{2u}[t], e_{6u}[t]$ and are characterized by variances $\sigma_{0u}^2, \sigma_{1u}^2, \sigma_{2u}^2, \sigma_{6u}^2$, respectively. The characteristic quantity can be the variance or the whiteness of the residual sequence as discussed in the following sections. The first subscript designates the model employed, while the second designates the aircraft state corresponding to the currently used response signal(s). The characteristic quantities obtained from the corresponding residual series are

[2]Bold–face upper/lower case symbols designate matrix/column–vector quantities, respectively. Matrix transposition is indicated by the superscript ^{T}.

designated as $Q_{0u}, Q_{1u}, Q_{2u}, Q_{6u}$. The characteristic quantities obtained using the baseline data records are designated as $Q_{VV}(V = 0, 1, 2, 6)$.

Residual Variance Method

In this method, the characteristic quantity used for fault detection is the residual variance (Ref. 8). Fault detection is based on the fact that the residual series $e_{0u}[t]$, obtained by driving the current signals Z_u through the model M_0 (corresponding to the healthy state) should be characterized by variance $\sigma^2_{0u} = \sigma^2_{00}$ which becomes minimal if and only if the current state of the aircraft is healthy ($Z_u = Z_0$). Fault detection is based on the following hypothesis testing procedure:

$$\begin{array}{lcll} H_0 & : & \sigma^2_{0u} \leq \sigma^2_{00} & \text{(null hypothesis – healthy aircraft)} \\ H_1 & : & \sigma^2_{0u} > \sigma^2_{00} & \text{(alternate hypothesis – rotor failure)} \end{array} \tag{8}$$

Under the null (H_0) hypothesis, the residuals $e_{0u}[t]$ are (just like the residuals $e_{00}[t]$), iid Gaussian with zero mean and variance σ^2_{00}. Hence the quantities $N_u \cdot \widehat{\sigma}^2_{0u}/\sigma^2_{00}$ and $(N_0 - d) \cdot \widehat{\sigma}^2_{00}/\sigma^2_{00}$ follow central χ^2 distribution with N_u and $N_o - d$ degrees of freedom, respectively (as sums of squares of independent standardized Gaussian random variables)[3]. N_0 and N_u designate the number of samples used in estimating the residual variance in the healthy and current cases, respectively (typically $N_0 = N_u = N$), and d designates the dimensionality of the estimated model parameter vector. N_u and N_0 should be adjusted to $N_u - 1$ and $N_0 - 1$, respectively, if each estimated mean is subtracted from each residual sequence. Consequently, the following statistic follows a Fischer distribution (denoted by F) with $(N_u, N_0 - d)$ degrees of freedom as the ratio of two independent and normalized χ^2 random variables (Ref. 8):

$$\text{Under } H_0 : F = \frac{\dfrac{N_u\ \widehat{\sigma}^2_{0u}}{N_u\ \sigma^2_{00}}}{\dfrac{(N_0 - d)\ \widehat{\sigma}^2_{00}}{(N_0 - d)\ \sigma^2_{00}}} = \frac{\widehat{\sigma}^2_{0u}}{\widehat{\sigma}^2_{00}} \tag{9}$$

The following hypothesis test is thus constructed at the α type I (false alarm) risk level:

$$\begin{array}{lcl} F \leq f_{1-\alpha}(N_u, N_0 - d) & \Longrightarrow & H_0 \text{ accepted (healthy aircraft)} \\ \text{Else} & \Longrightarrow & H_1 \text{ accepted (rotor failure)} \end{array} \tag{10}$$

where, $f_{1-\alpha}(N_u, N_0 - d)$ designates the corresponding Fischer distribution's $(1 - \alpha)$ critical point.

Fault identification may be similarly achieved via pairwise tests of the form:

$$\begin{array}{lcll} H_0 & : & \sigma^2_{Xu} \leq \sigma^2_{XX} & \text{(aircraft under Rotor X failure)} \\ H_1 & : & \sigma^2_{0u} > \sigma^2_{00} & \text{(aircraft not under Rotor X failure)} \end{array} \tag{11}$$

[3] A hat designates estimator/estimate of the indicated quantity; for instance $\widehat{\sigma}$ is an estimator/estimate of σ.

Residual Uncorrelatedness Method

This method is based on the fact that the residual series $e_{ou}[t]$, obtained by driving the current signals (Z_u) through the model (M_0), is uncorrelated (white) if and only if the aircraft is currently in its healthy condition (Ref. 8). Fault detection is performed by the following hypothesis testing:

$$\begin{array}{lcll} H_0 & : & \rho[\tau] = 0 & \text{(null hypothesis – healthy aircraft)} \\ H_1 & : & \rho[\tau] \neq 0 & \text{(alternate hypothesis – rotor failure)} \end{array} \tag{12}$$

where $\rho[\tau]$ is the normalized autocorrelation function ($\rho_{xx}[\tau] = \gamma_{xx}[\tau]/\gamma_{xx}[0]$) of the residual sequence $e_{0u}[t]$.

Therefore, the characteristic quantity for fault detection by this method is $\left[\rho[1]\ \rho[2]\ \rho[3] \ldots\ \rho[\tau]\right]^T$. For this method, r is the design variable for the statistical test, which denotes the maximum lag in time (τ) for which the normalized ACFs are being accounted for. Under the null hypothesis (H_0), the residuals $e_{0u}[t]$ are iid Gaussian with zero mean and the test statistic χ^2_ρ follows a χ^2 distribution with r degrees of freedom, given as:

$$\text{Under } H_0 : \chi^2_\rho = N(N+2) \cdot \sum_{\tau=1}^{r} (N - \tau)^{-1} \cdot \widehat{\rho}[\tau]^2 \sim \chi^2(r) \tag{13}$$

where $\widehat{\rho}[\tau]$ denotes the estimator of $\rho[\tau]$.

Statistical decision making is achieved by the following test for α (false alarm) risk level:

$$\begin{array}{lcl} \chi^2_\rho \leq \chi^2_{1-\alpha}(r) & \Longrightarrow & H_0 \text{ is accepted (healthy aircraft)} \\ \text{Else} & \Longrightarrow & H_1 \text{ is accepted (rotor failure)} \end{array} \tag{14}$$

where $\chi^2_{1-\alpha}(r)$ denotes the χ^2 distribution's $1 - \alpha$ critical point.

Fault identification is achieved by similarly examining which one of the $e_{Vu}[t](V = 1, 2, 6)$ residual series is statistically uncorrelated.

RESULTS AND DISCUSSION

Data Generation

Flight simulation for the hexacopter was performed at 5 m/s forward speed with under various turbulence levels according to the Dryden model. Figures 4 through 6 show attitude time histories for the hexacopter at 5 m/s forward flight, for cases of rotor 1 failure (red) and rotor 2 failure (green). For the simulation results presented, rotor failure (of either rotor 1 or 2) occurs at $t = 10$ s, indicated by the vertical dashed line.

From Fig. 4, it may be observed that rotor 1 failure results in a larger deviation in the pitch attitude than in the case of rotor 2 failure. In the case of front rotor failure, the hexacopter pitches down without any substantial change in roll angle (Fig. 5) because the loss of rotor 1 thrust does not significantly affect the aircraft roll equilibrium. However, in the case of side rotor failure (rotor 2) both the pitch (Fig. 4) and

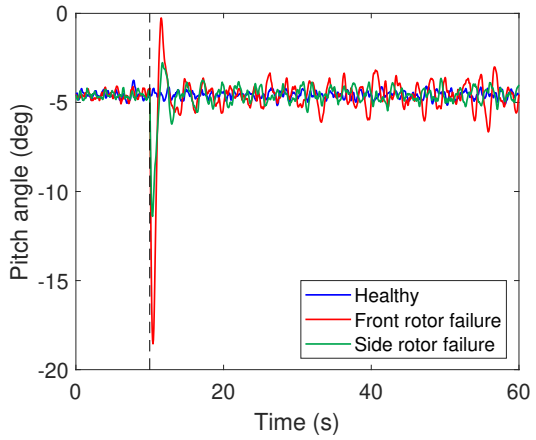

Fig. 4: Indicative pitch attitude signals for an airspeed of 5 m/s. The dashed vertical line indicates the time instant of the fault initiation.

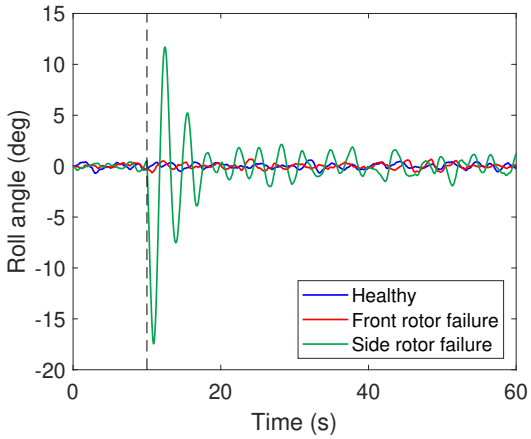

Fig. 5: Indicative roll attitude signals for an airspeed of 5 m/s.

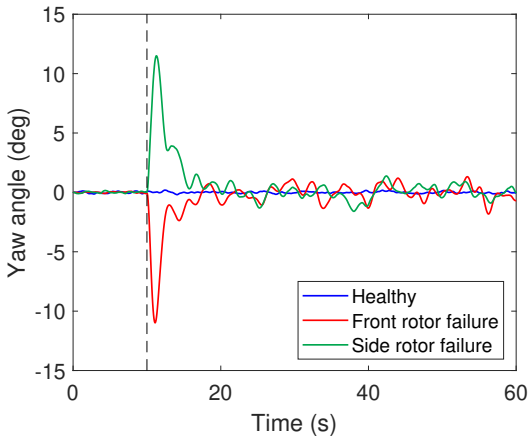

Fig. 6: Indicative yaw attitude signals for an airspeed of 5 m/s.

roll (Fig. 5) attitudes change and the roll attitude compensation is observed to be underdamped. In Fig. 6, the heading of the aircraft is observed to deviate in different directions with the failure of rotor 1 compared to rotor 2. This is due to the different rotor spin directions, and consequently the direction of the hub torque generated by each rotor.

It should be noted here that the signals show a transient response immediately after rotor failure followed by a fault-compensated steady state response where they become stationary again. Fig. 7 shows the variance of signals of window length 10 s, updated every 0.1 s. As the transients pass, the signal variance reduces considerably and becomes constant. This fact has been utilized to check whether steady state has been reached or not. The threshold values of variances for the roll, pitch and yaw signals, below which the signals are considered to have reached steady state, have been evaluated in the baseline phase as the maximum variances for each signal encountered in the steady state (20s after instant of rotor failure) for 20 sets of simulation data, for each type of rotor failure and severe level of turbulence. The value of roll, pitch, and yaw signals threshold variances are $1 \times 10^{-3} rad^2 (3.286\ deg^2)$, $1 \times 10^{-4} rad^2 (0.329 \quad deg^2)$ and $3 \times 10^{-4} rad^2 (0.986\ deg^2)$, respectively.

Due to different controller effort for the various levels of turbulence, the aircraft state signals do not show discernible change in characteristics with respect to the healthy dynamics, and transients due to failure and failure compensation under light and moderate levels of turbulence. Similar trends are observed for a flight speed of 10 m/s; the fault detection and identification process follows the same steps for any other speed. In the present study, indicative results for a single flight speed of 5 m/s are presented, results from various speeds will be presented in subsequent publication.

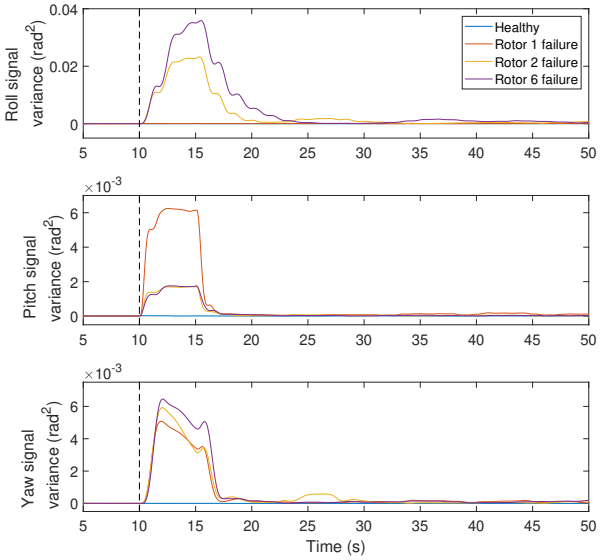

Fig. 7: Variance evolution of the roll, pitch and yaw signals. The dashed vertical line indicates the time instant of the fault initiation.

Parametric Model Identification

Scalar AR Model Identification Scalar (univariate) parametric identification of the aircraft dynamics has been based on 20 s ($N = 2000$ samples) of pitch signal obtained from the healthy aircraft flight at 5 m/s under severe levels of turbulence. In the present case, the response-only signals have been obtained from ambient excitation due to atmospheric turbulence (assumed to be uncorrelated based on the Dryden specifications). The model parameters and model order, a_i and na (Eq. 4), respectively, need to be estimated so that the model properly represents the dynamics of the system under healthy conditions. The modeling strategy consists of successive fitting of AR(na) models until a suitable model with least amount of complexity (number of parameters) and best fit is selected.

Model order selection is based on a combination of Bayesian Information Criteria (BIC) (Eq. 5) and Residual sum of squares normalized by Signal sum of squares (RSS/SSS) criteria (Eq. 6) as shown in Fig. 8. A model order of $na = 6$ yields the minimum BIC and this model is represented as AR(6). Monitoring the stabilization of RSS/SSS criteria gives the point where increasing model order does not result further in reduction of prediction errors. This order exhibits a very low RSS/SSS value of $1.6 \times 10^{-5}\%$ demonstrating accurate identification and excellent dynamics representation of the healthy aircraft pitch signal at 5 m/s and under severe turbulence. The number of parameters estimated for the AR(6) model results in a Samples per Parameter (SPP) ratio of 333.33 ($\frac{N}{d}$).

The model was validated based on the fact that the model matching the current state of the system should generate a white (uncorrelated) residual sequence. Therefore, a healthy pitch signal has been generated from a different realization of severe turbulence. The autocorrelation function of the residual sequences obtained from driving the current signal (healthy) through the model has been observed to be white with 95% confidence (confidence intervals shown in blue), as shown Fig. 9. Next, pitch signals generated under front and side rotor failures have been passed through the same model to generate residual sequences. Figure 9 shows that the residual sequences for different failure cases are serially correlated, demonstrating that the dynamics of the aircraft have changed from that of the healthy state, due to failure.

A similar study has been repeated with the roll and yaw signals to estimate scalar AR models for the healthy aircraft and different rotor failures, the details of which are given in Table 2. It should be noted that the models for different rotor failures are estimated with the stationary signals post fault compensation. A comparison of these models using various residual-based fault identification methods will be addressed with respect to their accuracy.

Vector AR Model Identification Vector (multivariate) parametric identification of the healthy aircraft has been based on 20 s ($N = 2000$ samples at sampling frequency 100 Hz) data sets for the roll, pitch, and yaw signals without any external

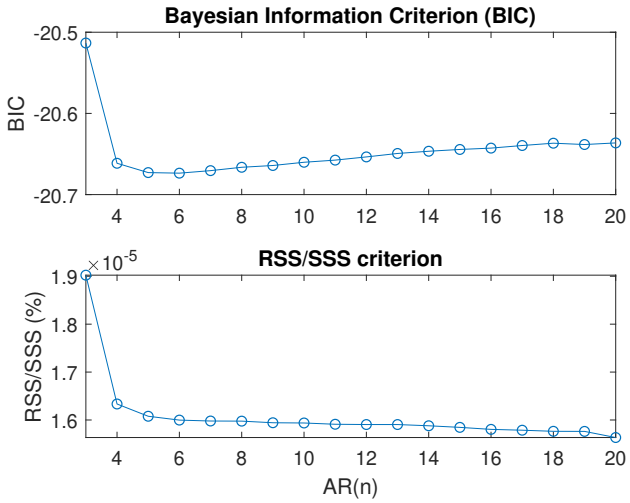

Fig. 8: Scalar AR model order selection criteria.

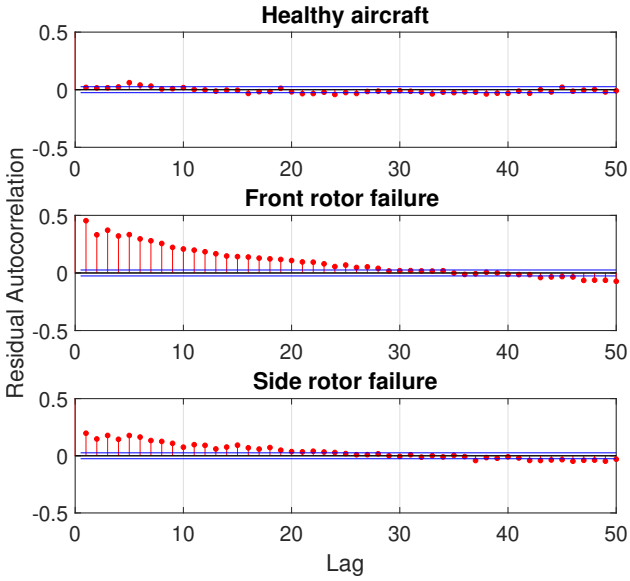

Fig. 9: Autocorrelation function of the pitch residual for the healthy and considered faulty rotor cases.

excitation (ambient excitation due to turbulence assumed to be white) generated from forward flight simulation at 5 m/s under severe turbulence. The model identification follows the same procedure as the scalar model to estimate the parameters $\boldsymbol{\theta}$ and select a model order na which can accurately represent the dynamics of the healthy aircraft.

The model order selection based on the BIC and RSS/SSS criteria yields yields a model order of 4, represented as VAR(4). The SPP for the model is 166.67 as the number of estimated parameters for VAR(4) is 36 (as the $\boldsymbol{A}_i$ parameter matrix is a 3×3 matrix with $i = 1,2,3,4$ for model order of 4). The roll, pitch, and yaw signals of the healthy aircraft flying at 5 m/s for different severe turbulence realization has been driven through the model estimated to generate residuals. The autocorrelation and cross-correlation functions of the three residual sequences generated are observed to be white with 95% confidence. For signals generated for different faulty states, the residuals are found to be correlated.

Table 2: Model identification summary results.

Aircraft State	Model type	Signals used	Model order	Parameters estimated	SPP
Healthy Aircraft	Scalar AR	Roll	AR(6)	6	333.33
		Pitch	AR(6)	6	333.33
		Yaw	AR(5)	5	400
	Vector AR	Roll,Pitch,Yaw	VAR(4)	36	166.67
Rotor 1 Failure	Scalar AR	Roll	AR(6)	6	333.33
		Pitch	AR(5)	5	400
		Yaw	AR(5)	5	400
	Vector AR	Roll,Pitch,Yaw	VAR(6)	54	111.11
Rotor 2 Failure	Scalar AR	Roll	AR(6)	6	333.33
		Pitch	AR(7)	7	285.71
		Yaw	AR(7)	7	285.71
	Vector AR	Roll,Pitch,Yaw	VAR(8)	72	83.33
Rotor 6 Failure	Scalar AR	Roll	AR(6)	6	333.33
		Pitch	AR(6)	6	333.33
		Yaw	AR(5)	5	400
	Vector AR	Roll,Pitch,Yaw	VAR(6)	54	111.11

Similarly, vector (multivariate) parametric identification of different rotor failure models have been based on 20 s ($N = 2000$ samples at sampling frequency 100 Hz) of steady state aircraft attitude signals after controller compensation obtained from forward flight simulation at 5 m/s under severe turbulence. Typically, the roll, pitch, and yaw signals fully stabilize with different dynamics than the healthy state due to controller action after rotor failure. The details of the estimated models for the healthy and all faulty states of the aircraft using the three aircraft attitude signals are given in Table 2.

Scalar Residual based Fault Detection and Identification

The current (unknown) pitch signals (5 m/s under severe turbulence) were driven through the identified healthy AR model to generate residual sequences. Fault detection was attempted through the characteristic quantities which are functions of the residual sequences, as previously discussed.

Similarly, in event of a rotor failure, fault identification was done via generating residuals from each of the rotor failure models and using their properties for decision making through multiple binary hypothesis tests. In the current study, the fault cases considered are failure of rotor 1, 2 and 6. Therefore, there are 3 fault hypothesis, and 3 hypothesis tests have to be carried out simultaneously.

Residual Variance Method Post online fault detection as discussed in (Ref. 6), the variance of the signals is monitored until steady state is reached. For fault identification, the current fault-compensated pitch signal of length 20 s ($N = 2000$ samples) updated every 1s is filtered through the scalar models identified with pitch signals of rotor failure 1,2 and 6. The residual variances denoted as σ^2_{1u},σ^2_{2u} and σ^2_{6u}, respectively, are statistically compared with the nominal values, namely σ^2_{11},σ^2_{22} and σ^2_{66}, estimated in the baseline phase. Indicative failure identification results for a single window is presented in Fig. 10. If the test statistic of the residual obtained from M_1 lies below the critical limit constructed at the α (false alarm) risk level of 10^{-12}, and exceeds for the residuals obtained from the other two models (M_2 and M_6) the fault is correctly identified as rotor 1 failure. Fault identification follows for the other types of failure in similar way. However, if the test statistics obtained from two or more models lie below the critical limit, then confusion between rotor failures is implied. If all the test statistics exceed the critical limit, no decision is made.

This method faces significant challenges for fault identification as it is not able to provide an accurate fault classification between all three rotor failures. This can be attributed to the fact that the pitch dynamics post failure have been compensated in similar fashion for all rotor failures by the controller, as discussed in (Ref. 6).

Residual Uncorrelatedness Method After the fault is compensated for by the controller, pitch signals of length 20 s ($N = 2000$ samples), updated every 1 s have been filtered through faulty models M_1, M_2, and M_6 to generate residuals $e_{1u}[t], e_{2u}[t]$ and $e_{6u}[t]$, respectively. The autocorrelation function of the residual sequences with maximum lag $\tau = 30$ has been considered as the characteristic quantity used to classify faults. The critical limit of a χ^2 distribution with 30 degrees of freedom for the statistical hypothesis testing has been constructed at the α (false alarm) risk level of 10^{-3}.

The results obtained from a single window of 20 s for different rotor failures have been shown in Fig.10. It can be observed that when pitch signal from rotor 1 failure is filtered through M_1, the residuals are uncorrelated, and they are correlated if obtained from models M_2 and M_6, as evident for the test statistic being below the critical limit in the former, and exceeding it in the latter two cases. In the case of the pitch signals for side (2 and 6) rotor failures, the residuals are correlated when filtered by M_1, signifying a clear distinction from front (1) ro-

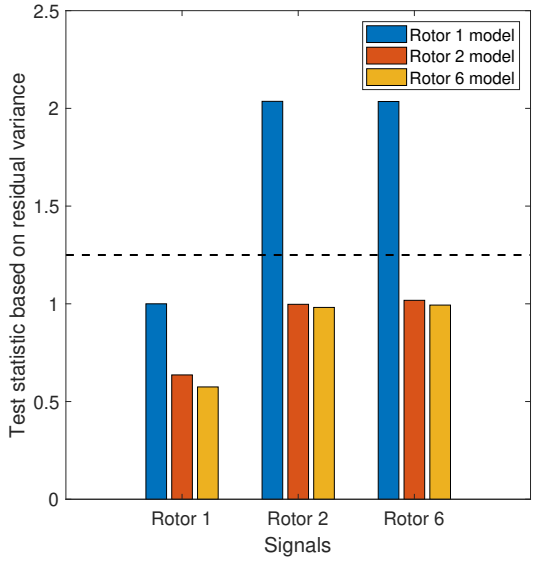

Fig. 10: Indicative pitch residual variance based fault identification results. The dashed black horizontal line indicates the statistical threshold at the $\alpha = 10^{-12}$ risk level.

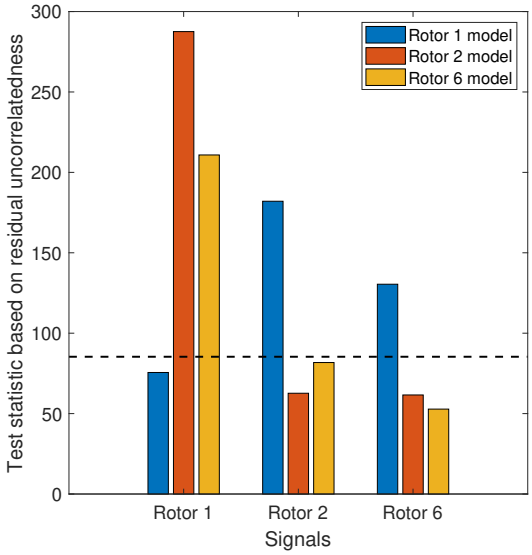

Fig. 11: Indicative pitch residual uncorrelatedness based fault identification results. The dashed black horizontal line indicates the statistical threshold at the $\alpha = 10^{-3}$ risk level.

tor failure. But, when filtered through models M_2 and M_6, they are not able to distinguish between the two side rotor failures, as the test statistics lie below the critical limit for both cases. This may be due to the fact that the pitch signals were compensated in different fashion for front and side rotor failures.

It should be noted that fault detection and identification is solely based on the response signals; in future work, the controller signals will be also taken into account to enhance the performance of the methods while taking into account the fault compensation characteristics of the controller.

Vector Residual based Fault Detection and Identification

The current (unknown) signals (roll, pitch and yaw, in that order), when driven through the VAR(4) model estimated in the "Vector AR Model Identification" section, yield three sets of residual sequences. The residual based fault detection is performed via the statistical comparison of each characteristic quantity obtained via the current residual sequence with the corresponding quantity obtained via the use of the baseline signals (signal used to estimate the healthy VAR model) and corresponding residual series through the baseline VAR model. In other words, the characteristic quantity obtained from the current roll residual sequence is compared to the baseline quantity obtained from the roll residual sequence. Therefore, the statistical hypothesis testing is performed thrice for a particular time window (duration of signal measured in number of samples).

For fault identification, the fault compensated signals are filtered through the 3 rotor failure models to generate 3 sets of residual sequences comprising of roll, pitch and yaw residuals. Binary hypothesis tests are designed on the properties of these residuals to decide whether the current faulty residuals are statistically similar to the which nominal rotor failure residuals (estimated during the baseline phase by filtering signals for a rotor failure through that particular rotor failure model).

Residual Variance Method After fault detection the variance of the signals are monitored to ascertain that steady state is reached. Post fault-compensation, the signals of length 20 s ($N = 2000$ samples), updated every 1 s have been filtered through the models for rotor failure, M_1, M_2, and M_6 to find the residual variances σ^2_{1u},σ^2_{2u}, and σ^2_{6u}, respectively (for roll,pitch and yaw residuals), and compare statistically to the baseline residuals σ^2_{11},σ^2_{22}, and σ^2_{66}. The statistical hypothesis test is designed at the α (false alarm) risk level of 10^{-8} to minimize the confusion between the various rotor failures.

Indicative results for a single signal window is presented in Fig. 12. If all the test statistics for the roll, pitch, and yaw residual sequences obtained from model M_1 are within the critical limit, then the fault is correctly classified as rotor 1 failure, as indicated in the left sub-figure. If any of them exceeds the critical limit, it is implied that the current faulty state is not related to rotor failure 1. Similarly, correct fault identification has been made with residuals obtained from models M_2 and M_6. If the test statistics of the residuals obtained from more than one model lie below the critical limit, it implies that there is confusion between those types of failures. Conversely, if all the test residuals from all the models exceed the critical limit, no decision is made on the type of rotor failure. As evident from the design of the test, multiple decisions or no decision is possible for a single window of the signals.

Residual Uncorrelatedness Method After the fault is compensated for by the controller, signals of length 20 s ($N = 2000$ samples), updated every 1 s have been filtered through faulty models M_1, M_2, and M_6 to generate residual sequences $e_{1u}[t], e_{2u}[t]$, and $e_{6u}[t]$, respectively, each containing roll, pitch, and yaw residuals. The autocorrelation function of

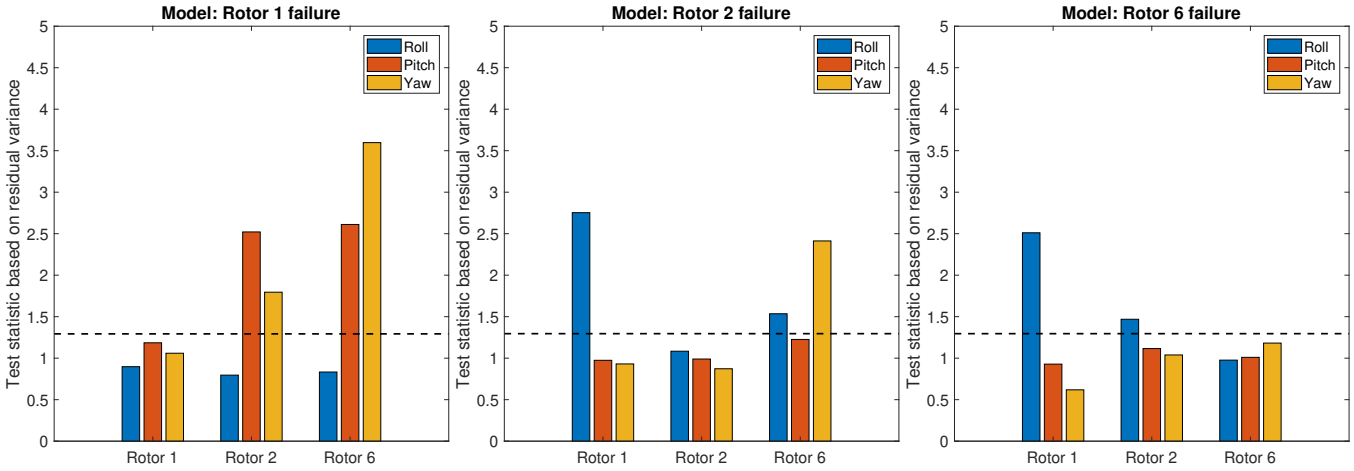

Fig. 12: Indicative residual variance based fault identification results. The dashed black horizontal line indicates the statistical threshold at the $\alpha = 10^{-8}$ risk level.

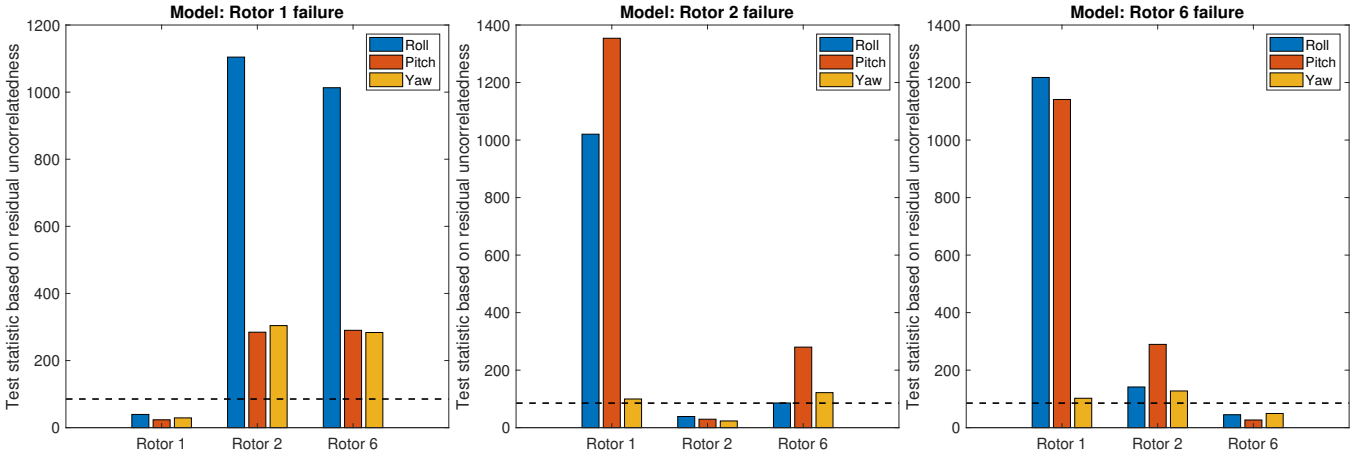

Fig. 13: Indicative residual uncorrelatedness based fault identification results. The dashed black horizontal line indicates the statistical threshold at the $\alpha = 10^{-3}$ risk level.

each component of the residual sequences with maximum lag $\tau = 50$ has been considered as the test statistics to classify faults. Since the computation time required to classify failure is about 0.3 s, the window update interval is kept at 1 s.

The results obtained from a single window of 20 s are shown in Fig.13. Figure on the left shows the residuals $e_{1u}[t]$ are uncorrelated (lies below $(1-\alpha)$ critical limit of a χ^2 distribution with 50 degrees of freedom). This signifies that the model (M_1) represents the dynamics of current state correctly and hence the fault is classified as failure of rotor 1. The models which do not represent the current aircraft state dynamics, have correlated residuals (exceed the critical limit). Similarly, the middle and right figures, show correct identification of the failure for rotors 2 and 6, respectively. Note that the roll statistic (blue bar) shows a clear distinction between the front and side rotor failure cases.This is due to the fact that roll does not change significantly for front rotor failure as captured by model M_1, contrary to the case of side rotor failure. Also, the front rotor failure signals show a substantial pitch correlation compared to the other side rotor failure, which signifies that controller compensated pitch dynamics is significantly different in front rotor failure from side rotor failure, as previously discussed in Ref. 6.

Comparative Assessment of Different Models and Fault Identification Methods

It has been observed that both scalar and vector statistical time series methods have shown remarkable results in effectively detecting faults, with the vector methods achieving improved performance with respect to false alarms, missed faults and distinguishing between healthy and faulty compensated states (Ref. 6). This can be attributed to the fact that vector models being multivariate models can capture the relationship between all three aircraft output states. Similarly for the task of fault identification, a similar difference in performance between these two types of models is observed.

Table 3 outlines the type I risk level (α) selected for each residual based fault identification method based on the achieved effectiveness and robustness. If α is not properly

Table 3: Parameters used for various fault identification methods

Model type	Fault identification method	α level
Scalar AR	Residual variance	10^{-6}
Roll	Residual whiteness	10^{-3}
Scalar AR	Residual variance	10^{-12}
Pitch	Residual whiteness	10^{-3}
Scalar AR	Residual variance	10^{-12}
Yaw	Residual whiteness	10^{-3}
Vector AR	Residual variance	10^{-8}
Roll, Pitch, Yaw	Residual whiteness	10^{-3}

α: Type I (false alarm) error probability level

adjusted, the methods may exhibit decreased accuracy and robustness with respect to the probability of false alarms and misclassification faults. Hence, it is advised to make an initial investigation on the number of false alarms for different levels of turbulence using several healthy data sets. Then, misclassification errors may be checked with data corresponding to various rotor failure states. Moreover, for robust performance of parametric methods, a very small value of the type I risk (α) is often required. This is due to the fact that the stochastic time series models (like AR, ARMA, ARX, state space, etc.) used for modeling the dynamics are still incapable of fully capturing the experimental, operational and environmental uncertainties that the aircraft may be subjected to. Therefore, to "compensate" for the lack of effective uncertainty modeling, a very small α is often selected. Another important factor is the number of samples needed for hypothesis testing, since the chance of missing faults depends upon sample size.

Table 4 summarizes the accuracy of the different methods and models for fault identification aggregated over severe, moderate, and low levels of turbulence. Each column shows the percentage of time the signals from a particular rotor failure has been classified as rotor (1) / rotor (2) / rotor (6) failure.

Scalar AR models estimated with fault-compensated stationary signals for each type of rotor failure, namely rotor 1, 2, and 6, failures are mostly rendered ineffective in fault identification as shown in Table 4. AR models identified based on roll signals can only distinguish between front rotor (1) and side rotor (2 and 6) failures using the residual uncorreladtedness method with accuracy of 96% due to difference in fault dynamics (see discussion in "Data Generation"). The remaining scalar AR methods for classifying rotor failures show considerable confusion between all 3 rotor failures.

Vector AR models estimated for different rotor failures model the relationship between the fault-compensated roll, pitch and yaw signals. Hence, they have the potential to perform better than their scalar counterparts in fault identification due to the fact the the signal inter-dependencies and cross-correlation structure is taken into account.

Vector AR models with residual uncorrelatedness based decision making perform excellent in fault identification. It has been observed that signal length 20 s gives failure classification accuracy of 99.6%, however the accuracy reduces significantly with shorter signal lengths, with the confusion between rotor 2 and 6 failures (classified as both failures simultaneously) up to 56% when signal lengths of 5 s are used for online monitoring. On the other hand, the residual variance method, though able to distinguish between front and side rotor failure with an accuracy of 100%, suffers from considerable confusion (31.26%) and inability to make a correct decision (80%) in the case of side rotor (2 or 6) failures.

The residual uncorreladtedness method compares a function of the residual autocorrelation for a properly defined lag value τ, specified by the user, and holds more information compared to residual variance method which only compares the variance of the signals with the nominal values. It is possible for the variance values to be statistically similar for several fault types. However, autocorrelation function can take positive and negative values for different lags and it being similar for different rotor failures is improbable due to the fact that the dynamics of the system changes in markedly different way for different rotor failures. This fact has been exploited in another study (Ref. 7), where the difference between the correlation functions of the signal residuals obtained from VAR model of healthy aircraft for different rotor failures, have been utilized for more accurate fault identification.

CONCLUSIONS

This paper presented the application and assessment of several residual-based statistical time series methods for online rotor fault detection and identification in multicopters under different levels of atmospheric turbulence and uncertainty. Development of various types of statistical time series models (scalar and vector) to represent healthy and post failure fault compensated aircraft dynamics have been discussed. Different fault identification methods coupled with the models estimated have been compared with respect to their accuracy and robustness. The important conclusions from the study are summarized below.

- Statistical time series methods for rotor fault detection and identification in multicopters achieve effective detection based on (i) ambient (white) excitation and aircraft state (*scalar* or *vector*) signals, (ii) statistical model building, and (iii) statistical decision making under uncertainty.

Table 4: Fault identification accuracy of different methods

Model type	**Fault identification method**	**Signals for Failure of**		
		Rotor (1)	Rotor (2)	Rotor (6)
Scalar AR	Residual Variance	97.54/100/99.36	0/100/100	0/100/100
Roll	Residual Whiteness	98.78/0.23/1.19	0/97.06/99.20	0/97.38/97.93
Scalar AR	Residual Variance	100/0/0	100/100/100	100/100/100
Pitch	Residual Whiteness	87.70/7.38/10.95	56.90/98.25/98.96	86.18/98.57/98.89
Scalar AR	Residual Variance	100/14.76/0.32	100/94.52/59.04	100/99.28/95.95
Yaw	Residual Whiteness	77.77/46.02/42.85	58.77/49.04/45.47	88.09/60.79/56.58
Vector AR	Residual Variance	100/0/0	0/21.75/0	0/31.26/33.49
Roll,Pitch,Yaw	Residual Whiteness	100/0/0	0/99.62/0.02	0/0/99.68

Identification as Rotor (1)/ Rotor (2)/ Rotor (6) failure in percentage
for all levels of turbulence out of 20 datasets each

- Both parametric methods have great sensitivity to faults and accuracy of detection when fault occurs in real time, with the vector methods achieving improved performance with respect to false alarms, missed faults and distinguishing between healthy and faulty compensated states.
- Fault identification by statistical time series method requires multiple models for different rotor failures. Decision making takes longer time as the hypothesis tests increase with number of fault classes and types. Also, the accuracy of this method depends on the length of current signals (number of samples). Using longer signals (and thus greater sample size) has been observed to result in improved accuracy.
- Fault identification by scalar methods has shown considerable confusion in distinguishing between the various rotor failures. Roll signals via the residual uncorrelatedness method provide good distinction between front and side rotor failures, but have been proven worse for missing front rotor failure in detection phase.
- Fault identification via the use of vector models and the residual uncorrelatedness method achieves the best fault classification accuracy. The residual variance method achieves good distinction between the front and side rotor failures, but is unable to classify between the two side rotor failures.
- In the future, the modeling will be expanded to Functionally Pooled (FP) model based methods that will include various forward flight speeds and gross weight of the aircraft into a single 'global' model for complete rotor fault detection (abrupt failure and continuous degradation), identification.

AUTHOR CONTACT INFORMATION

Airin Dutta duttaa5@rpi.edu
Michael McKay mckaym2@rpi.edu
Fotis Kopsaftopoulos kopsaf@rpi.edu
Farhan Gandhi fgandhi@rpi.edu

REFERENCES

[1]M. Frangenberg, J. Stephan, and W. Fichter, "Fast Actuator Fault Detection and Reconfiguration for Multicopters," in *AIAA Guidance, Navigation, and Control Conference*, AIAA, Jan. 2015.

[2]G. Heredia and A. Ollera, "Sensor Fault Detection in Small Autonomous Helicopters using Observer/Kalman Filter Identification," in *IEEE International Conference on Mechatronics, Malaga, Spain*, IEEE, Apr. 2009.

[3]M. McKay, R. Niemiec, and F. Gandhi, "Post-Rotor-Failure-Performance of a Feedback Controller for a Hexacopter," in *American Helicopter Society 74th Annual Forum, Phoenix, AZ*, AHS, May 2018.

[4]V. Stepanyan, K. Krishnakumar, and A. Bencomo, "Identification and Reconfigurable Control of Impaired Multi-Rotor Drones," in *AIAA Science and Technology Forum and Exposition*, Jan. 2016.

[5]X. Qi, D. Theillol, J. Qi, Y. Zhang, and J. Han, "A Literature Review on Fault Diagnosis Methods for Manned and Unmanned Helicopters," in *2013 International Conference on Unmanned Aircraft Systems*, May 2013.

[6]A. Dutta, M. McKay, F. Kopsaftopoulos, and F. Gandhi, "Rotor Fault Detection and Identification on a Hexacopter Based on Statistical Time Series Methods," in *Vertical Flight Society 75th Annual Forum, Philadelphia, PA*, AHS, May 2019.

[7]A. Dutta, M. McKay, F. Kopsaftopoulos, and F. Gandhi, "Fault Detection and Identification for Multirotor Aircraft by Data-Driven and Statistical Learning Methods," in *Electric Aircraft Technologies Symposium (EATS), Indianapolis, IN*, AIAA/EATS, August 2019.

[8]S. Fassois and F. Kopsaftopoulos, *New Trends in Structural Health Monitoring*, ch. Statistical Time Series Methods for Vibration Based Structural Health Monitoring, pp. 209–264. Springer, Jan. 2013.

[9]F. P. Kopsaftopoulos and S. D. Fassois, "Scalar and Vector Time Series Methods for Vibration Based Damage Diagnosis in a Scale Aircraft Skeleton Structure ," *Journal of Theoretical and Applied Mechanics*, vol. 49, no. 4, 2011.

[10]P. A. Samara, G. N. Fouskitakis, J. S. Sakellariou, and S. D. Fassois, "A Statistical Method for the Detection of Sensor Abrupt Faults in Aircraft Control Systems," *IEEE Transactions on Control Systems Technology*, vol. 16, pp. 789–798, July 2008.

[11]F. P. Kopsaftopoulos and S. D. Fassois, "A vibration model residual-based sequential probability ratio test framework for structural health monitoring," *Structural Health Monitoring*, vol. 14, no. 4, pp. 359–381, 2015.

[12]D. G. Dimogianopoulos, J. D. Hios, and S. D. Fassois, "FDI for Aircraft Systems Using Stochastic Pooled-NARMAX Representations: Design and Assessment," vol. 17, pp. 1385–1397, Nov. 2009.

[13]D. Peters and C. He, "A Finite-State Induced Flow Model for Rotors in Hover and Forward Flight," in *American Helicopter Society 43rd Annual Forum, St. Louis, MO*, AHS, May 1987.

[14]T. M. I. Hakim and O. Arifianto, "Implementation of Dryden Continuous Turbulence Model into Simulink for LSA-02 Flight Test Simulation," in *Journal of Physics: Conference Series 1005(2018) 012017*, Aug. 2018.

[15]E. L. Lehmann and J. P. Romano, *Testing Statistical Hypotheses*. Springer, 3rd ed., 2008.

[16]G. E. P. Box, G. M. Jenkins, and G. C. Reinsel, *Time Series Analysis: Forecasting & Control*. Prentice Hall: Englewood Cliffs, NJ, third ed., 1994.

[17]L. Ljung, *System Identification: Theory for the User*. Prentice–Hall, 2nd ed., 1999.

[18]S. D. Fassois, "Parametric identification of vibrating structures," in *Encyclopedia of Vibration* (S. Braun, D. Ewins, and S. Rao, eds.), pp. 673–685, Academic Press, 2001.

[19]T. Söderström and P. Stoica, *System Identification*. Prentice–Hall, 1989.

[20]H. Lütkepohl, *New Introduction to Multiple Time Series Analysis*. Springer-Verlag Berlin, 2005.